Available online at www.sciencedirect.com

ScienceDirect

Procedia Materials Science 3 (2014) 110 – 115

Procedia Materials Science

www.elsevier.com/locate/procedia

20th European Conference on Fracture (ECF20)

About the influence of line-shaped inclusions on the path of fatigue cracks

Gunter Kullmer*, Britta Schramm, Hans-Albert Richard

Institute of Applied Mechanics, Faculty of Mechanical Engineering, University of Paderborn, Pohlweg 47-49, 33098 Paderborn, Germany

Abstract

Secure findings on the propagation behavior of fatigue cracks are essential for the evaluation of the safety of components and structures. Therefore the growth of cracks in the vicinity of material boundaries, whereas also accidental inclusions represent such material boundaries, has to be considered, too. Depending on the way an initial crack enters the region of influence of such a material boundary, the crack may grow towards or away from the material boundary. In both cases a curved crack path results that cannot be explained with the global loading but obviously with different stiffness relations.

Selection and peer-review under responsibility of the Norwegian University of Science and Technology (NTNU), Department of Structural Engineering

Keywords: Curved crack path; crack growth simulation; accidental inclusion; material inclusion; finite elements

1. Introduction

An important topic of the Collaborative Research Centre TRR 30 of the Deutsche Forschungsgemeinschaft (DFG) is the crack propagation behavior in graded materials. Also the growth of cracks in the neighborhood of material boundaries belongs under this topic. Whereas accidentally embedded extraneous material may represent such material boundaries. Depending on the way a crack penetrates the zone of influence of the material boundary the crack may grow towards or away from the material boundary. Both cases result in curved crack paths that cannot be explained only with the global loading situation. Curved crack paths result from mixed mode loading at the crack

* Corresponding author. Tel.: +49-5251-60-5320; fax: +49-5251.60-5322
E-mail address: kullmer@fam.upb.de

Selection and peer-review under responsibility of the Norwegian University of Science and Technology (NTNU), Department of Structural Engineering
doi:10.1016/j.mspro.2014.06.021

tip. Thereby in general the basic crack opening modes, see Fig. 1, tensile opening (mode I), in-plane shear (mode II) and anti-plane shear (mode III) co-occur.

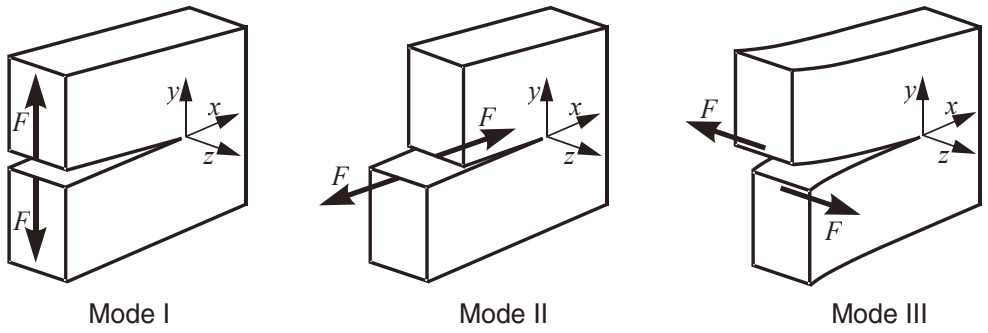

Fig. 1. Basic crack opening modes, Richard and Sander (2009)

Whereas a crack propagates self-similar under mode I loading it deflects under mode II loading about the angle φ_0 and twists under mode III loading about the angle ψ_0, see Fig. 2. Under superposition of all three modes the crack simultaneously deflects and twists, see Fig. 2. Under plane mixed mode with continuously changing ratios of mode I and mode II curved cracks form in the x-y-plane according to Fig. 1.

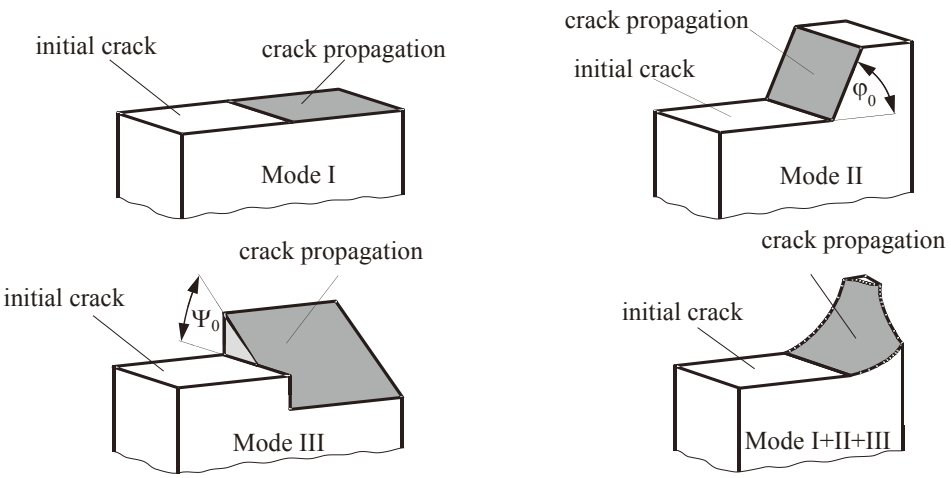

Fig. 2. Crack propagation under different crack opening modes, Richard and Sander (2009)

2. FE-model for the simulation of fatigue crack propagation in the vicinity of inclusions

Simulation models based on the CT-specimen are used to investigate basically the influence of line-shaped inclusions with different stiffness and different orientation on the path of fatigue cracks. As shown in Fig. 3 a rectangular partition is inserted into the CAD-model of the CT-specimen to represent the line-shaped inclusion. The undefined dimensions are chosen $a_0/w = 0.2$ and $c/w = 0.3$. The thickness is 5mm. To investigate the principle influence of a different stiffness of the inclusion on the crack path Young´s modulus of the inclusion is once chosen twice and once chosen half the Young´s modulus of the base material. Furthermore the rectangular partition is rotated in discrete steps of 10° from 30° to 90° as well as 45° about the centre A of the rectangle to analyse the influence of the inclusion orientation in relation to a global mode I-loading of the starting crack.

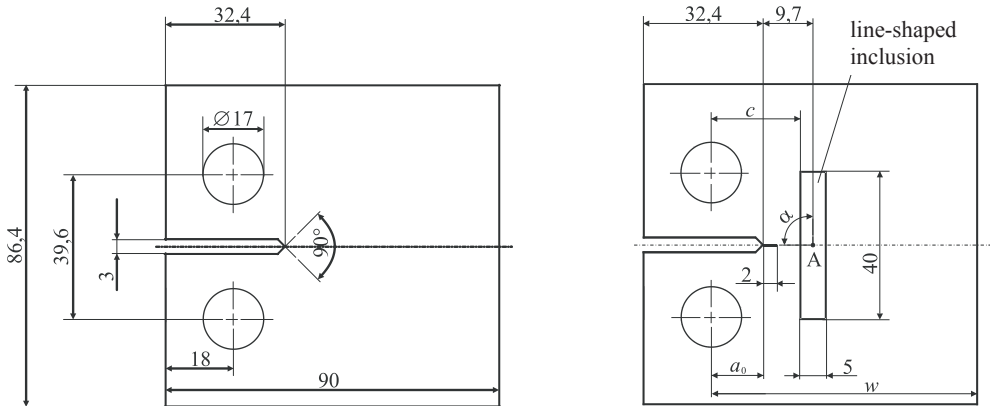

Fig. 3. Geometry of the CT-specimen and positioning of the line-shaped inclusion

The CT-specimen is partitioned according to Fig. 4. Partitions P1 and P2 consist of the base material whereas partition P3 consists of the inclusion material. Partition P2 guarantees a comparable fine mesh in the neighborhood of partition P3 and identical boundary conditions independent from the orientation angle α of the inclusion. Therefore the boundaries of partition P2 are sufficiently distant from partition P2 for all investigated orientations of the inclusion.

Furthermore Fig. 4 shows the boundary conditions. All simulation models are supported at the positions A, B and C. The bearing is statically determined and symmetrical. The specimen is loaded with distributed loads with a resulting load of 12.5kN. The boundary conditions are chosen in a way that the bearing reactions vanish and symmetrical deformation occurs if all partitions consist of the same material.

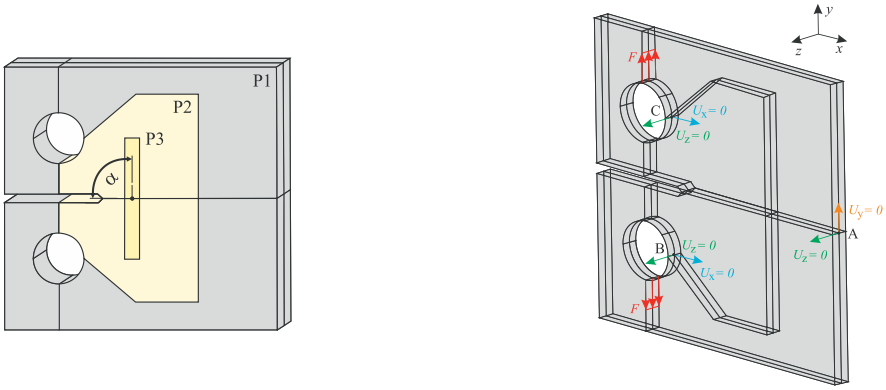

Fig. 4. Partitioning of the CT-specimen and definition of the boundary conditions

The material behavior in all partitions is idealized linear elastic, isotropic and homogeneous. Within the partitions P1 and P2 Young´s modulus is $210.000\,N/mm^2$. Young´s modulus in partition P3 is $420.000\,N/mm^2$ for the stiff inclusion and $105.000\,N/mm^2$ for the compliant inclusion. Poisson´s ratio is zeroed to avoid stress in thickness direction of the specimen and to assure a state of plane stress although a three-dimensional FE-model is used. A three-dimensional model is required since the crack growth is simulated with the program system ADAPCRACK3D developed by the Institute of Applied Mechanics of the University of Paderborn (Fulland 2003).

Fig. 5 shows a typical global mesh exemplary for the CT-specimen with an inclusion orientation of 45°. The mesh consists of 10-noded quadratic tetrahedral elements. Within the partitions P2 and P3 where the crack most likely will propagate the edge length of the elements is chosen 1mm whereas in partition P1 an edge length of 2.5mm is sufficient.

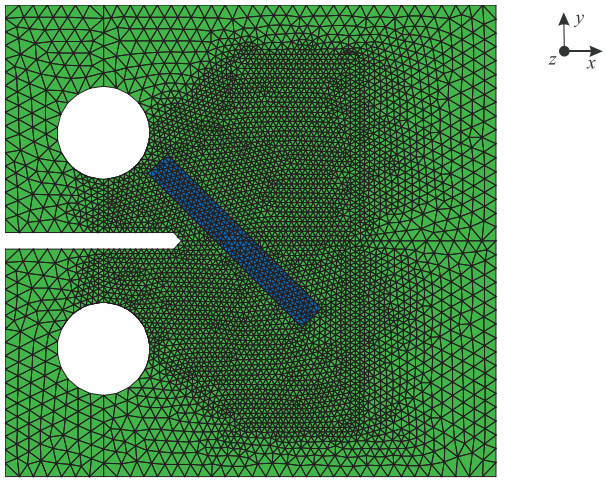

Fig. 5. Exemplary mesh for the CT-specimen with an inclusion orientation of 45°

For the crack growth simulation with ADAPCRACK3D the global mesh is unstitched along the crack path with the aid of a crack model. The crack model is a surface mesh that contains only the surface of the crack. At first the crack model is built up of the mesh of the initial crack as shown in Fig. 6. Therefore linear triangle elements with an edge length of 0.5mm are used. The initial crack has a lateral length of 2mm as defined in Fig. 3. For a growing crack the crack model is incrementally extended with additional crack surfaces in the direction depending on the estimated mixed mode ratio. Since the present investigation in principle represents a plane problem Poisson´s ratio is zeroed to provide a state of plane stress and the stress intensity factor K_{III} is neglected to avoid a twisting of the crack surface. Furthermore ADAPCRACK3D is modified in a way that with every simulation step a uniform crack increment over the specimen thickness with a fixed lateral length is provided.

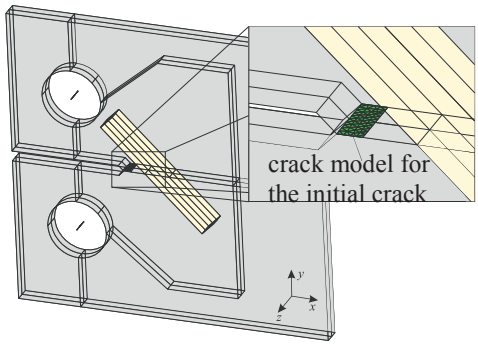

Fig. 6. Positioning of the crack model within the CT-specimen, orientation of the inclusion $\alpha = 45°$

For the calculation of the stress intensity factors K_I und K_{II} for the actual crack state ADAPCRACK3D uses the modified virtual crack closure integral (MVCCI) after Rybicki and Kanninen 1977 applied to a comoving submodel composed of a regular linear hexahedral mesh containing the crack front. Since plane mixed mode loading is existent the crack deflection angles are calculated with the maximum tangential stress criterion after Erdogan and Sih 1963.

For the verification of the simulation model and the modified version of ADAPCRACK3D three CT-specimens with inclusions with an orientation angle of 90° are analyzed. Young´s modulus of the inclusion is chosen half, double and equal to Young´s modulus of the base material. Due to symmetry the crack should grow straight through the inclusion independent of the stiffness of the inclusion. The resulting crack paths for all three cases are almost straight with a maximum deviation from the straight line of clearly less than 0.1mm. Thus the simulation model and

the modified version of ADAPCRACK3D are suitable for the intended investigation. Moreover the CT-specimen with an inclusion orientation of 45° is simulated with crack growth increments of 0.2mm, 0.5mm und 1mm. Because the resulting crack paths are almost the same the fixed standard crack increment of 0.5mm for the further simulations is a reasonable compromise between time and effort.

3. Results of the crack growth simulations

The simulated crack paths for the different orientations of the inclusion and the alignment of the inclusion for the extreme orientation angles $\alpha = 30°$ as well as $\alpha = 90°$ are presented in Fig. 7.

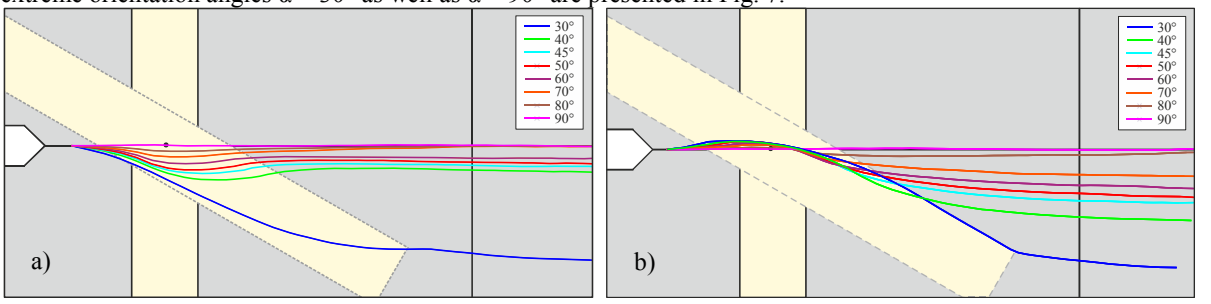

Fig. 7. Simulated crack paths with variable orientation of the inclusion, a) stiff inclusion, b) compliant inclusion

For $\alpha = 90°$ the crack propagates independently of the inclusion stiffness straight through the inclusion. With increasing inclination angle of the inclusion the deflection of the crack rises. If the crack penetrates the region influenced by the stiffness mismatch of an inclined inclusion it tends to grow around the boundary to the stiff material and to grow towards the boundary to the compliant material. This can be clearly seen with the simulation results for the inclusion with orientation angle $\alpha = 30°$. If the crack traverses the inclusion the crack growth behavior reverses approaching the second material boundary. When the crack leaves the region influenced by the stiffness mismatch the crack approaches tangentially a parallel to the extension line of the initial crack. The offset of the parallel to the extension line increases with the inclination of the inclusion. Where the crack crosses a material boundary the crack path has a turning point and the curvature of the path changes. This means that the stress intensity factor K_{II} is zero at the material boundary and the crack locally grows straight under mode I conditions. The maximal magnitude of K_{II} corresponds with the maximal curvature of the crack path and the maximal stiffness mismatch due to the inclusion. Anyway K_{II} is small compared to K_I. The qualitative development of K_I is shown in Fig. 8 with a bubble diagram whereupon the bubble diameter represents the magnitude of K_I.

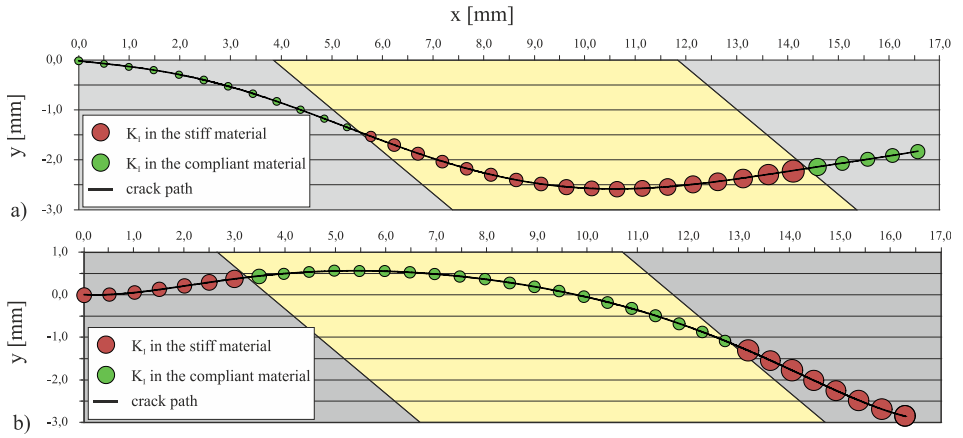

Fig. 8. Bubble diagram of K_I along the crack path through the inclusion with $\alpha = 40°$, a) stiff inclusion, b) compliant inclusion

If the crack approaches a boundary to stiff material K_I slightly reduces although the crack length increases and the load stays constant. Apparently the stiff material region causes a stress shield for the crack tip. If the crack approaches a boundary to compliant material K_I increases. At the entrance into the stiff region K_I increases about the factor $\sqrt{2}$ whereas at the entrance into the compliant region K_I decreases about the factor $\sqrt{2}$. Since with linear-elastic material behavior the relation $K_I = \sqrt{G_I E}$ is valid and at the material boundaries Young´s modulus E changes about the factor 2 obviously the energy release rate is constant when the crack crosses the material transition.

4. Conclusions

The comparison of the crack paths for stiff and for compliant inclusions shows that in both cases at the material transition from compliant to stiff the crack tends to go around the material boundary and thus reduces the transition angle as defined in Fig. 9. At the material transition from stiff to compliant the crack tends to grow towards the material boundary and thus increases the transition angle. As shown in Fig. 10 the transition angles are equal for similar material transitions.

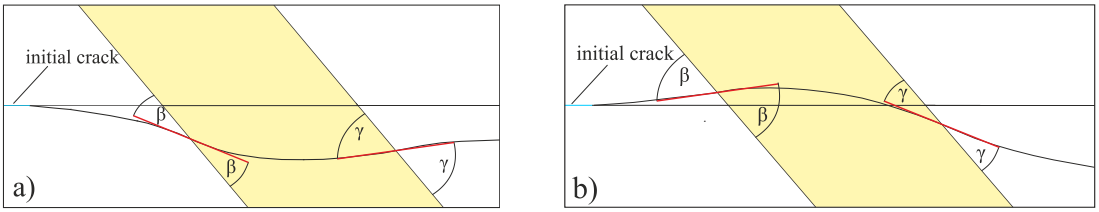

Fig. 9. Definition of the crack entrance angle β and the crack exit angle γ, a) stiff inclusion, b) compliant inclusion

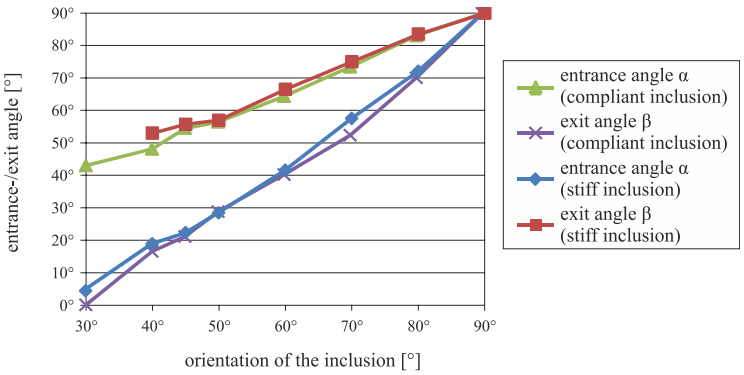

Fig. 10. Comparison of the entrance- and exit angles depending on the stiffness of the inclusion

Both cases of material transitions result in curved crack paths with turning points at the material boundary. Obviously the amount of the stiffness mismatch of the material regions and the angle between the initial crack and the material boundary are responsible for the curvature of the crack path.

References

Richard, H. A., Sander, M., 2009. Ermüdungsrisse. Vieweg+Teubner Verlag, Wiesbaden

Fulland, M., 2003. Risssimulationen in dreidimensionalen Strukturen mit automatischer adaptiver Finite-Elemente-Netzgenerierung. Fortschritt-Bericht VDI, Reihe 18: Mechanik/Bruchmechanik Nr. 280, VDI-Verlag, Düsseldorf

Rybicki, E. F., Kanninen, M. F., 1977. A Finite Element Calculation of Stress Intensity Factors by a modified Crack Closure Integral. Engineering Fracture Mechanics 9, 931-938

Erdogan, F., Sih, G. C., 1963. On the crack extension in plates under plane loading and transverse shear. Journal of Basic Engineering 85, 519-525